DALTON

Crystal structures, electronic properties and structural pathways of four [Cu(phen)$_2$Cl][Y] complexes (phen = 1,10-phenanthroline; Y = $BF_4^-\cdot 0.5H_2O$, PF_6^-, $CF_3SO_3^-\cdot H_2O$ or BPh_4^-)†

Gillian Murphy, Pat Nagle, Brian Murphy and Brian Hathaway*

The Chemistry Department, University College Cork, Ireland

The crystal structures of [Cu(phen)$_2$Cl][BF_4]·0.5H_2O **1** (phen = 1,10-phenanthroline), [Cu(phen)$_2$Cl][PF_6] **2**, [Cu(phen)$_2$Cl][CF_3SO_3]·H_2O **3** and [Cu(phen)$_2$Cl][BPh_4] **4** have been determined by X-ray crystallography. Three of the complexes, **1**–**3**, involve a CuN_4Cl chromophore with a square based pyramidal distorted trigonal bipyramidal stereochemistry, while **4** involves a trigonal bipyramidal distorted square based pyramidal stereochemistry. The geometries of the CuN_4Cl chromophores in **1**–**4** were compared by scatter-plot analysis with those of four other [Cu(phen)$_2$Cl][Y] complexes of known structure. The scatter plots of the eight cation distortion isomers of the [Cu(phen)$_2$Cl][Y] complex suggest that all the complexes involve a −A + B route distortion of the CuN_4Cl chromophore, −A (*ca.* 60%) and +B (*ca.* 40%), The observation of linear and parallel correlations are alternatively interpreted as a direct observation of vibronic coupling of a mixture of the symmetric, ν_{sym}, C_2 mode and the asymmetric, ν_{asym}, non-C_2 mode of vibration of the CuN_4Cl chromophore. This emphasises the need to determine the structure of more than one complex in a series of cation distortion isomers, in which the limits of the range of stereochemistries are indicated by the measurement of the electronic reflectance spectra.

The concept of a structural pathway[2,3] for [Cu(chelate ligand)$_2$X][Y] type complexes has recently been developed for nine complexes of the [Cu(bipy)$_2$Cl]$^+$ cation[1] (bipy = 2,2′-bipyridyl) using scatter plots, Fig. 1. The present paper examines the consequences of changing the chelate ligand from bipy to phen (1,10-phenanthroline), to form a corresponding series of [Cu(phen)$_2$Cl][Y] complexes, where phen is a more rigid bidentate nitrogen chelate ligand than bipy. The structures of four [Cu(phen)$_2$Cl][Y] complexes,[4–6] **5**–**8**, are already known and this paper reports the preparation and crystal structure determination of four additional [Cu(phen)$_2$Cl]$^+$ cation distortion isomers, **1**–**4**.

Experimental

Preparations

The complex [Cu(phen)$_2$Cl][BF_4]·0.5H_2O **1** was prepared by adding a boiling solution of phen (0.46 g, 2.55 mmol) in methanol (200 cm^3) to a boiling solution of Cu(BF_4)$_2$·6H_2O (0.44 g, 1.27 mmol), $H_2NOH\cdot HCl$ (0.2 g, 2.88 mmol) and 0.88 mol dm^{-3} NH_4OH (1 cm^3) in water (20 cm^3). The resulting red copper(I) solution was filtered and left to oxidise slowly in air. Green crystals of **1** were deposited after several days and were filtered off and dried at the pump (Found: C, 52.15; H, 2.9; Cl, 6.25; Cu, 11.15; N, 10.15. Calc. for $C_{24}H_{17}BClCuF_4N_4O_{0.5}$: C, 51.6; H, 3.05; Cl, 6.25; Cu, 10.05; N, 10.1%).

The complex [Cu(phen)$_2$Cl][PF_6] **2** was prepared by mixing boiling solutions of $CuCl_2$·2H_2O (0.2 g, 2.6 mmol) in water (80 cm^3) and phen (0.47 g, 2.6 mmol) in ethanol (80 cm^3) with KPF_6 (0.24 g, 1.3 mmol). The resulting precipitate was recrystallised from acetonitrile–1,3-dimethoxypropane (5:1, 60 cm^3) and yielded green crystals of **2** (Found: C, 48.05; H, 3.05; Cl, 6.05; Cu, 10.05; N, 8.95. Calc. for $C_{24}H_{16}ClCuF_6N_4P$: C, 47.7; H, 2.65; Cl, 5.85; Cu, 10.5; N, 9.25%).

The complex [Cu(phen)$_2$Cl][CF_3SO_3]·H_2O **3** was prepared by mixing a hot solution of phen (0.36 g, 2 mmol) in propanone (150 cm^3) with a hot aqueous solution (30 cm^3) of Cu(CF_3SO_3)$_2$ (0.36 g, 1 mmol) and NaCl (0.06 g, 1 mmol). The resulting solution yielded turquoise needles after 1 d (Found: C, 48.2; H, 2.9; Cl, 5.55; Cu, 9.75; N, 9.45. $C_{25}H_{18}ClCuF_3N_4O_4S$ requires C, 47.95; H, 2.9; Cl, 5.65; Cu, 10.15; N, 8.95%).

The complex [Cu(phen)$_2$Cl][BPh_4] **4** was prepared by adding a hot solution of phen (0.36 g, 2 mmol) in acetonitrile (300 cm^3) to a hot aqueous solution (20 cm^3) of $CuCl_2$·2H_2O (0.17 g, 1 mmol). A hot aqueous solution (10 cm^3) of $NaBPh_4$ (0.34 g, 1 mmol) was then added. Large olive-green crystals were obtained after 1 d (Found: C, 73.8; H, 4.7; Cl, 4.6; Cu, 8.15; N, 6.95. $C_{48}H_{36}BClCuN_4$ requires C, 74.05; H, 4.65; Cl, 4.55; Cu, 8.15; N, 7.2%).

Crystallography

The crystallographic data for complexes **1**–**4** are summarised in Table 1. For **1** and **2** the unit-cell data (25 reflections, θ 3–25°) and the intensity data were collected at 298 K on a Philips PW 1100 four-circle diffractometer with graphite-monochromatised Mo-Kα radiation (λ = 0.710 69 Å). An ω–2θ scan mode was used with reflections in the range 3 < θ < 25° and in one quarter of the reciprocal lattice space. A constant scan speed of 0.05° s^{-1} was used with a variable scan width of (0.7 + 0.1 tan θ). The acceptance criterion $I > 2.5\sigma(I)$ was used. Lorentz-polarisation corrections were applied, but no correction was made for absorption.

The unit-cell parameters of complexes **3** and **4** were determined and the intensity data collected on an Enraf-Nonius CAD4 diffractometer. Reflections in the range 3.0 < θ < 24° in one hemisphere were collected for both complexes. The data were collected at room temperature. A constant scan speed of 7° min^{-1} was used with a variable scan width (0.8 + 0.2 tan θ). Other details as above.

All four structures were solved by Patterson and Fourier techniques, developed by Fourier difference techniques, ($|F_o| - |F_c|$), and refined by full-matrix least-squares analysis, with the $\Sigma w(|F_o| - |F_c|)^2$ function minimised, and initially $w = 1/[\sigma^2(F_o)]$. Anisotropic thermal parameters were used on all the non-hydrogen atoms. The positions of the hydrogen atoms were calculated geometrically, with C–H and O–H distances of 1.08 Å, and floated on the associated carbon or oxygen atom with a fixed thermal parameter of 0.07 Å^2. Finally, a refined weighting

† Comparative crystallography. Part 3.[1]

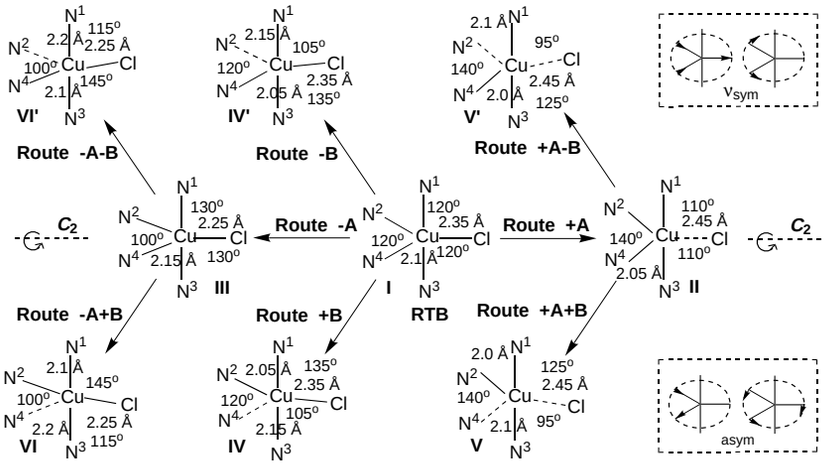

Fig. 1 The forms of distortion of the RTB CuN_4Cl chromophore involving the ±A, ±B and ±A ± B routes (bond distances are rounded off to the nearest 0.05 Å)

Table 1 Crystallographic and structure refinement data for $[Cu(phen)_2Cl][BF_4]\cdot 0.5H_2O$ **1**, $[Cu(phen)_2Cl][PF_6]$ **2**, $[Cu(phen)Cl][CF_3SO_3]\cdot H_2O$ **3** and $[Cu(phen)Cl][BPh_4]$ **4**

	1	**2**	**3**	**4**
Formula	$C_{24}H_{17}BClCuN_4F_4N_4O_{0.5}$	$C_{24}H_{16}ClCuF_6N_4P$	$C_{25}H_{18}ClCuF_3N_4O_4S$	$C_{48}H_{36}BClCuN_4$
M	554.8	603.4	626.5	778.6
Crystal system	Monoclinic	Monoclinic	Triclinic	Triclinic
Space group	$P2_1/c$ (C_{2h}^5, no. 14)	$P2_1/c$ (C_{2h}^5, no. 14)	$P\bar{1}$ (C_i^1, no. 2)	$P\bar{1}$ (C_i^1, no. 2)
a/Å	12.507(4)	12.973(4)	10.349(2)	11.177(3)
b/Å	11.493(4)	11.127(4)	12.111(2)	11.423(1)
c/Å	17.246(5)	17.499(5)	12.379(2)	15.514(2)
α/°			61.65(2)	87.08(1)
β/°	111.08(3)	110.73(3)	79.11(1)	76.63(1)
γ/°			65.99(2)	78.45(1)
U/Å^3	2313.16	2362.52	1247.20	1888.03
Z	4	4	2	2
D_c/g cm^{-3}	1.59	1.70	1.62	1.37
F(000)	1132	1212	614	806
μ/cm^{-1}	10.63	11.13	10.71	6.50
No. unique reflections (*N*)	2603	2842	3739	5575
No. varied parameters (*P*)	317	398	353	497
N/*P*	8.21	7.14	10.59	11.22
R	0.0731	0.0610	0.0532	0.0485
R′	0.0785	0.0674	0.0565	0.0474
k	1.0000	0.3853	1.0000	37.6548
g	0.005 172	0.013 114	0.044 245	0.000 356
Maximum final shift/e.s.d.	0.010	0.005	0.010	0.020
Residual electron density/e Å^{-3}	+0.89, −1.27	+0.75, −1.30	+0.59, −0.88	+0.34, −0.44
No. atoms with anisotropic thermal parameters	36	37	39	55

scheme was introduced with $w = k/[\sigma^2(F_o) + g(F_o)^2]$ (see Table 1 for the final values of *k* and *g*).

The $[BF_4]^-$ anion of complex **1** was disordered and refined as a rigid body with fixed B–F and F ··· F distances of 1.370 and 2.237 Å, respectively. Attempts to refine the $[BF_4]^-$ anion as two disordered interpenetrating BF_4 groups were unsuccessful. The highest residual electron density in **1** was associated with the disordered $[BF_4]^-$ anion and probably accounts for the relatively high *R* value of 0.073. Complex neutral atom scattering factors were used for the non-hydrogen atoms and for the Cu, Cl and P atoms.[7]

All calculations were carried out with the SHELX 76,[8] SHELX 86,[9] XANADU,[10] PUBTAB[11] and XCAD[12] programs on an VAX 6310 mainframe computer; PLUTON 92[13] was run on a Memorex 386 personal computer.

Selected bond lengths and angles for the eight $[Cu(phen)_2Cl][Y]$ complexes are given in Table 2. Fig. 2 shows a representative molecular structure for the $[Cu(phen)_2Cl]^+$ cation, the atom numbering scheme and the angle notation used.

Atomic coordinates, thermal parameters, and bond lengths and angles have been deposited at the Cambridge Crystallographic Data Centre (CCDC). See Instructions for Authors, *J. Chem. Soc., Dalton Trans.*, 1997, Issue 1. Any request to the CCDC for this material should quote the full literature citation and the reference number 186/553.

The diffuse reflectance spectra in the range 5000–30 000 cm^{-1} were measured as polycrystalline samples on a Shimadzu UV–VIS 3101 spectrometer.

Results and Discussion

Crystal structures

The crystal structures of complexes **1**–**4** consist of discrete $[Cu(phen)_2Cl]^+$ cations and $[BF_4]^-$, $[PF_6]^-$, $[CF_3SO_3]^-$ and $[BPh_4]^-$ anions, respectively. In addition **1** and **3** involve molecules of water in the unit cell, 0.5 and 1.0 mol, respectively. None of the anions or water molecules is close enough (<3.0 Å) to be considered even weakly semi-co-ordinated to the copper(II) cation.[14] The cations all involve a five-co-ordinate CuN_4Cl chromophore, with a near trigonal bipyramidal stereochemistry having a square based pyramidal distor-

Table 2 Selected bond lengths (Å) and angles (°) for the [Cu(phen)$_2$Cl][Y] complexes

	Y							
	BF_4·0.5H_2O **1**	ClO_4 **5**[4]	PF_6 **2**	Cl·1.5H_2O·$(CH_3)_2CO$ **6**[5]	NO_3·H_2O **7**[6]	Cl·1.5H_2O·$(CH_3)_2CO$ **8**[5]	CF_3SO_3·H_2O **3**	BPh_4 **4**
Cu–N(Cl)*	2.014(2)	2.008(2)	2.004(2)	1.991(1)	2.002(1)	1.967(1)	1.990(1)	1.964(1)
Cu–Cl	2.304(2)	2.298(2)	2.294(2)	2.281(1)	2.292(1)	2.257(1)	2.280(1)	2.254(1)
Cu–N(1)	1.995(6)	1.986(6)	2.001(4)	1.999(4)	1.988(4)	1.990(4)	1.998(2)	2.024(2)
Cu–N(2)	2.078(5)	2.077(6)	2.076(4)	2.126(3)	2.091(2)	2.108(2)	2.127(2)	2.057(2)
Cu–N(3)	2.011(6)	2.004(6)	2.003(4)	1.995(3)	1.989(4)	1.993(4)	1.996(2)	2.008(2)
Cu–N(4)	2.121(6)	2.136(6)	2.157(4)	2.138(3)	2.132(2)	2.151(4)	2.151(2)	2.242(2)
α_1	126.6(2)	127.6(2)	131.6(1)	130.4(1)	135.8(1)	133.0(1)	138.7(1)	157.7(1)
α_2	118.9(2)	119.0(2)	114.4(1)	129.6(1)	119.2(1)	120.6(1)	127.9(1)	105.9(1)
α_3	114.5(2)	113.4(2)	114.1(2)	100.0(1)	105.0(1)	106.4(1)	93.4(1)	96.4(1)
α_4	92.8(2)	92.3(2)	93.4(1)	94.1(1)	92.7(1)	96.8(1)	93.2(1)	92.7(1)
α_5	91.2(2)	90.9(2)	91.0(1)	95.0(1)	91.8(1)	94.2(1)	94.6(1)	91.4(1)
α_6	81.3(2)	81.7(2)	81.0(2)	80.1(2)	81.4(1)	81.1(1)	80.7(1)	81.0(1)
α_7	80.6(2)	80.5(2)	80.1(2)	80.5(1)	80.8(1)	80.6(2)	80.2(1)	79.2(1)
α_8	175.3(2)	176.2(2)	175.2(2)	170.8(1)	175.6(1)	168.6(2)	172.1(1)	169.2(1)
α_9	98.1(2)	98.2(2)	97.5(2)	95.1(2)	95.8(1)	93.8(1)	92.8(1)	91.5(1)
α_{10}	95.4(2)	96.0(2)	96.3(2)	92.5(1)	96.5(1)	91.0(2)	95.7(1)	109.1(1)
τ	0.81	0.81	0.73	0.67	0.66	0.59	0.56	0.19

* The Cu–Cl distances are corrected to Cu–N values using the relationship Cu–Cl − 0.29 Å = Cu–N(Cl).

Table 3 Maxima, minima, difference (Δ) and average values of the bond lengths (Å) and angles (°) for the [Cu(phen)$_2$Cl][Y] complexes

	Cu–Cl	Cu–N(Cl)	Cu–N(1)	Cu–N(2)	Cu–N(3)	Cu–N(4)	τ
Maximum	2.304(2)	2.014(2)	2.024(2)	2.127(2)	2.011(6)	2.242(2)	0.81
Minimum	2.254(1)	1.964(1)	1.986(6)	2.057(2)	1.989(4)	2.121(6)	0.19
Δ	0.050	0.050	0.038	0.070	0.022	0.121	0.62
Average	2.283(1)	1.993(1)	1.998(4)	2.093(3)	2.000(4)	2.154(4)	

	α_1	α_2	α_3	α_4	α_5	α_6	α_7	α_8	α_9	α_{10}
Maximum	157.7(1)	129.6(1)	114.5(2)	96.8(1)	95.0(1)	81.7(2)	80.8(1)	176.2(2)	98.2(2)	109.1(1)
Minimum	126.6(2)	105.9(1)	93.4(1)	92.3(2)	90.9(2)	80.1(2)	79.2(1)	168.6(2)	91.5(1)	91.0(2)
Δ	31.1	23.7	21.1	4.5	4.1	1.6	1.6	7.6	6.7	18.1
Average	135.2(1)	119.4(1)	105.4(1)	93.5(1)	92.5(1)	81.0(2)	80.3(1)	172.9(2)	95.4(2)	96.6(2)

tion[1] (SBPDTB) in **1**, **2** and **3**, and a trigonal bipyramidal distorted square based pyramidal stereochemistry (TBDSBP) for **4**. All four complexes are further examples of distortion isomers of the $[Cu(phen)_2Cl]^+$ cation, whose stereochemistries are related by the structural pathways[1] of Fig. 1. No attempt will be made to describe the individual structures of complexes **1**–**4**, Table 2, but scatter-plot analysis will be used to compare their structures with those of four [Cu(phen)$_2$Cl][Y] complexes of known crystal structure.[4–6] Table 2 summarises the selected bond lengths and angles of all eight complexes, sequenced in order of their τ values, where $\tau = (\alpha_8 - \alpha_1)/60$,[15] and Table 3 summarises the maximum, minimum, difference (Δ) and average bond length and angle values for the series of eight [Cu(phen)$_2$Cl][Y] complexes. Table 4 gives the sums of the in-plane angles, α_{1-3}, and distances, Cu–N(2), Cu–N(4) and Cu–Cl.

The [Cu(phen)$_2$Cl][Y] data

The structures of the eight five-co-ordinate CuN_4Cl chromophores vary from near TB to near SBP, reflected in a range of τ values[15] of 0.81 to 0.19, $\Delta\tau = 0.62$. This is a substantial variation in τ, the largest seen to date for cation distortion isomers of the [Cu(chelate ligand)$_2$X][Y] series of complexes.[1] None of the complexes has a near-RTB (regular trigonal bipyramidal) stereochemistry or a two-fold axis of symmetry. Seven complexes have τ values in the more limited range of 0.81 to 0.56 and their stereochemistries are best described as SBPDTB. Complex **4** has a τ value of 0.19 and a stereochemistry best described as TBDSBP.

Relative to a RTB stereochemistry, the out-of-plane distances, Table 2, show only small differences, Table 3, with ΔCu–N(1) = 0.038 Å and ΔCu–N(3) = 0.022 Å. The largest variations in bond lengths are present in the equatorial bond distances Cu–Cl, Cu–N(2) and Cu–N(4), respectively. The Cu–N(4) distances show the largest variation ranging from 2.121(6) to 2.242(2) Å, with $\Delta = 0.121$ Å and average = 2.154(4) Å. The Cu–N(2) distances vary from 2.057(2) to 2.127(2) Å, with $\Delta = 0.070$ Å and average = 2.093(3) Å. The Cu–Cl distances range from 2.254(1) to 2.304(2) Å, with $\Delta = 0.050$ Å and average = 2.283(1) Å. The average of the in-plane Cu–N(2,4) distances, 2.124(4) Å, is greater than the average of the axial Cu–N(1,3) distances, 1.999(4) Å, by 0.125 Å, consistent with a TB stereochemistry and slightly greater than the difference of 0.1 Å normally observed,[16] which is probably associated with the exceptionally large value of the Cu–N(4) distance of 2.242(2) Å for complex **4**.

The out-of-plane bond angles, Table 2, show only small differences, Table 3, with $\Delta\alpha_{4-7}$ ranging from 1.6 to 4.5° but with the α_{8-10} angles showing larger differences than expected, 7.6–18.1°. The α_1 in-plane angles show the largest variation ranging from 126.6(2) to 157.7(1)°, with $\Delta = 31.1°$ and average = 135.2(1)°. The α_2 angles vary from 105.9(1) to 129.6(1)°, with $\Delta = 23.7°$ and average = 119.4(1)°. The α_3 angles show the smallest variation ranging from 93.4(1) to 114.5(2)°, with $\Delta = 21.1°$ and average = 105.4(1)°.

From Table 2 it is noticeable that within the range of τ values of 0.81–0.19 there is a significant gap of 0.37 in τ value between the extreme TBDSBP value of 0.19 for **4** and the next highest

Table 4 Sums of the in-plane bond angles and distances for the $[Cu(phen)_2Cl][Y]$ complexes

	Complex							
	1	**5**	**2**	**6**	**7**	**8**	**3**	**4**
α_1/°	126.6	127.6	131.6	130.4	135.8	133.0	138.7	157.7
α_2/°	118.9	119.0	114.4	129.6	119.2	120.6	127.9	105.9
α_3/°	114.5	113.4	114.1	100.0	105.0	106.4	93.4	96.4
Sum/°	360.0	360.0	360.1	360.0	360.0	360.0	360.0	360.0
Cu–Cl/Å	2.304	2.298	2.294	2.281	2.292	2.257	2.280	2.254
Cu–N(2)/Å	2.078	2.077	2.076	2.126	2.091	2.108	2.127	2.057
Cu–N(4)/Å	2.121	2.136	2.157	2.138	2.132	2.151	2.151	2.242
Sum/Å	6.503	6.511	6.527	6.545	6.515	6.516	6.558	6.553

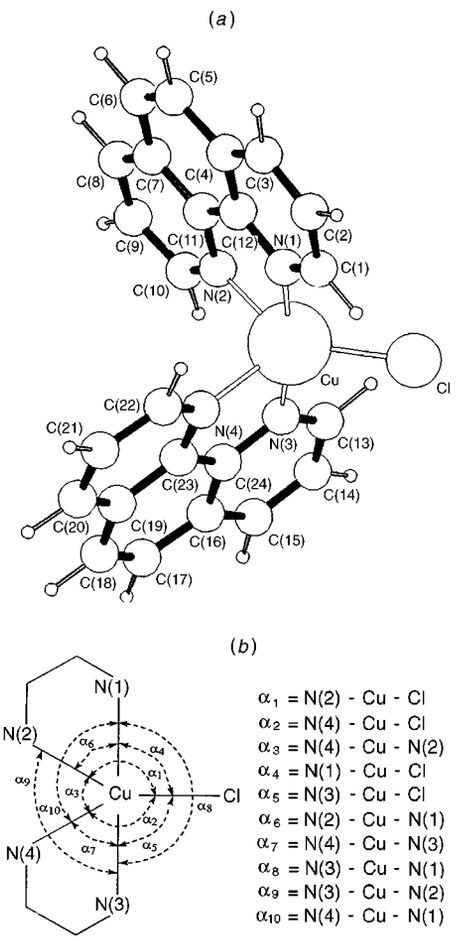

Fig. 2 (*a*) The molecular structure of the $[Cu(phen)_2Cl]^+$ cation of complex **3**; (*b*) the atom numbering scheme and α_n notation for the CuN_4Cl chromophore

value of 0.56 for **3**. This gap corresponds with a change in the ratio of the α_9 and α_{10} angles, for τ values > 0.56, $\alpha_9 > \alpha_{10}$, but for τ values < 0.56, $\alpha_9 < \alpha_{10}$. Equally, while the phen ligand is constrained to be essentially planar, with angles between the pyridine rings of 0–5°, in complex **4** both of these angles are less than 1.02°. This suggests that once formed the geometry of the TBDSBP stereochemistry is inherently more stable, than the range of SBDTB stereochemistries, τ 0.56–0.81, a stability that could be locked in place by the essential planarity of the phen ligand. This is also reflected in the near trigonal α_1 angles of 126.6–138.7° of the SBPDTB stereochemistries, relative to an α_1 angle of 157.7° in **4**.

Scatter-plot analysis for the $[Cu(phen)_2Cl][Y]$ complexes

This section presents the data for the $[Cu(phen)_2Cl][Y]$ complexes, Table 2, using scatter-plot analysis. The scatter plots

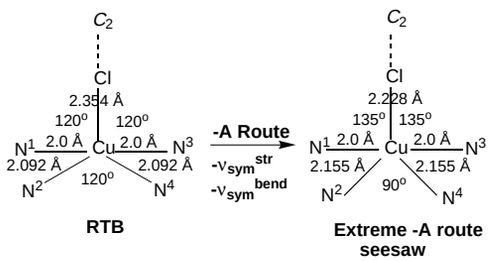

Fig. 3 Distortion of the CuN_4Cl chromophore from RTB to an extreme −A route or 'seesaw' stereochemistry

discussed are as follows: (*a*) τ *versus* Cu–N(4), (*b*) α_3 *versus* α_1, (*c*) α_3 *versus* Cu–Cl and (*d*) Cu–N(2) *versus* Cu–N(4). An overview of the range of stereochemistries is provided by the plot of τ *versus* Cu–N(4). However, as τ involves two simultaneous angle changes, it will not be used further. A number of suggested extreme data points, Table 5, are included in the plots, with the geometry of the extreme 'seesaw' stereochemistry illustrated in Fig. 3.

The eight data points in Fig. 4(*a*) vary from near regular trigonal bipyramidal, RTB, to near regular square based pyramidal, RSBP, with the τ values decreasing from 0.81 to 0.19 as the Cu–N(4) distances increase from 2.121(6) to 2.242(2) Å. The data points show a broad *inverse* trend, and clearly do not cluster about RTB. This plot provides an overview of the observed stereochemistries of the $[Cu(phen)_2Cl][Y]$ complexes as a whole. There are no data points at RTB ($\tau = 1.0$), but there is one data point, **4**, with an exceptionally low τ value of 0.19 at near SBP. Seven of the eight data points have τ values in the range 0.81 to 0.56. The main correlation involving the RTB and RSBP data points contains one data point, **1**, with the remaining seven data points lying nearby. To confirm the exceptional structure of **4** the crystallographic data have been independently recollected[17] at 150 K. There were no significant differences in the room temperature and the 150 K structures and also the low-temperature structure confirms that the stereochemistry of **4** is a static non-fluxional stereochemistry[3] of the copper(II) cation.

The data points in Fig. 4(*b*) show the α_3 values decreasing from 114.5(2) to 93.4(1)° as the α_1 values increase from 126.6(2) to 157.7(1)°. All eight data points have α_1 values >120° and α_3 values <120°, Table 2. All eight data points are found in the −A +B section of the graph, with one data point **6** lying very close to the pure −A pathway. There are no data points on the RTB ⟶ + A or on the RTB ⟶ RSBP (−A + B) distortion pathways. Four data points, **1**, **5**, **7** and **8**, and the RTB data point, show an *inverse* trend. Each of these data points has α_2 120 ± 1°. The remaining data points, **3**, **6**, **2** and **4**, lie on possible parallel correlations (- - -) displaying α_2 values of 130, 130, 115 and 105°, consistent with $\alpha_1 + \alpha_2 + \alpha_3 = 360°$, Table 4, and possibly suggesting the occurrence of preferred or 'magic angles'. This series of four possible parallel correlations (- - -) have the same slopes. The data points show a SBP distortion,

Table 5 Limiting values for the ±A, +B, −A + B and +A + B route distortions

	RTB	+A (RSBP)	−A (seesaw)	+B	−A + B (RSBP)	+A + B (RSBP)
α_1 /°	120	97.5	135	150	165	105
α_2 /°	120	97.5	135	90	105	90
α_3 /°	120	165	90	120	90	165
Cu−N(4)/Å	2.092	1.998	2.155	2.199	2.262	2.025
Cu−N(2)/Å	2.092	1.998	2.155	1.985	2.048	1.971
Cu−Cl/Å	2.354	2.543	2.228	2.354	2.228	2.543

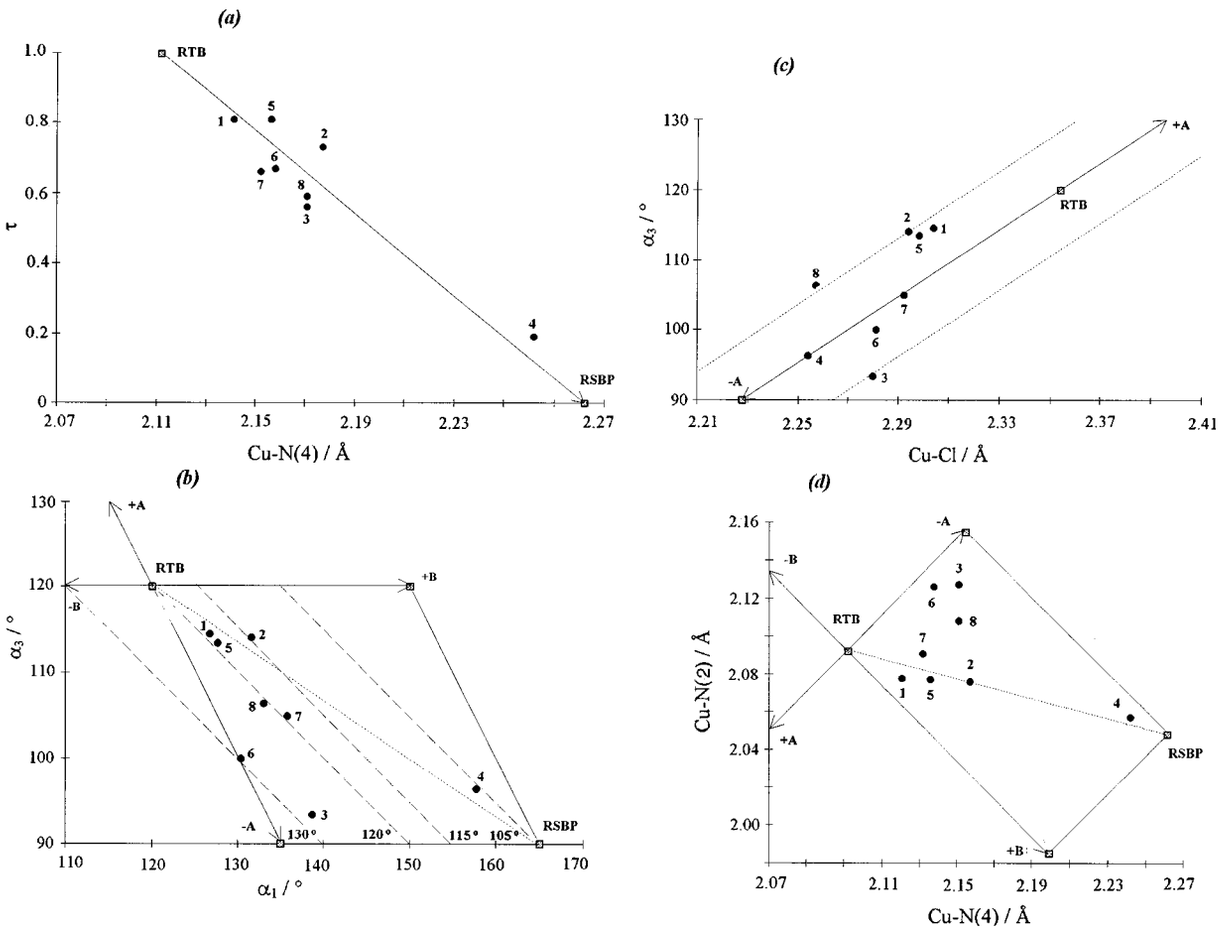

Fig. 4 Standard scatter plots for the $[Cu(phen)_2Cl][Y]$ complexes

but only the correlation with an α_2 value of 105° can correlate with the RSBP data point. For these parallel correlations, the α_2 values remain constant, therefore $\Delta\alpha_1\uparrow \approx \Delta\alpha_3\downarrow$. The % −A and % +B distortion values calculated from the in-plane α_1 and α_3 bond angle data of Fig. 4(*b*) are shown in Table 6.

The eight data points in Fig. 4(*c*) show the α_3 values decreasing from 114.5(2) to 93.4(1)° as the Cu−Cl distances decrease from 2.304(2) to 2.254(1) Å. All the data points have α_3 values <120° and Cu−Cl distances <2.354 Å. There is a *normal* correlation involving two data points, **7** and **4**, connecting the RTB data point to the extreme 'seesaw'[18] data point (the −A route distortion, SSDTB, Fig. 3). There is a parallel correlation involving four data points, **1**, **2**, **5** and **8**, which have α_3 values 9° higher than the corresponding points on the RTB ⟶ − A correlation (data point **7** has $\alpha_3 = 105.0°$, while data point **2**, lying almost directly above it on the parallel correlation, has $\alpha_3 = 114.1°$). An isolated data point, **3**, may lie on another parallel correlation, since it has an α_3 value 9° lower than the corresponding point on the RTB ⟶ − A correlation.

If the data of Fig. 4(*c*) are related to those of Fig. 1, then both the α_3 angles and the Cu−Cl distances correspond to a pure −A route distortion of the RTB stereochemistry. In practice, the α_1 and α_2 angles are not even approximately equal, varying from $\Delta(\alpha_1 - \alpha_2) = 7.7–51.8°$, Table 2. An exceptional data point **6**, with $\Delta(\alpha_1 - \alpha_2) = 0.8°$, does not lie on any of the three lines, but with an α_3 value of 100.0° represents the most extreme, but distorted, near 'seesaw' structure of the $[Cu(phen)_2Cl][Y]$ complexes. The extreme −A route distortion is clearly five-co-ordinate, with three short bonds, Cu−N(1) = Cu−N(3) ≈ 2.0 Å, Cu−N(Cl) ≈ 2.05 Å, and two longer bonds, Cu−N(2) = Cu−N(4) ≈ 2.15 Å, with in-plane angles of $\alpha_1 = \alpha_2 = 135$ and $\alpha_3 = 90°$. The best description of this unique extreme −A route distortion is a five-co-ordinate 'seesaw' stereochemistry,[18] SSDTB, Fig. 3. In general, in view of the non-equivalence of the α_1 and α_2 angles and the Cu−N(2) and Cu−N(4) distances, the two-fold axis of symmetry of the pure −A route distortion is not appropriate and there must also be a corresponding +B route distortion occurring, which cannot be observed from this graph.

The data points in Fig. 4(*d*) show the Cu−N(2) distances decreasing from 2.127(2) to 2.057(2) Å, as the Cu−N(4) distances increase from 2.121(6) to 2.242(2) Å. All eight data

Table 6 The % −A and % +B distortion values of the complexes calculated using the in-plane angle data of Fig. 4(*b*)

	Complex							
	1	**5**	**2**	**6**	**7**	**8**	**3**	**4**
% −A	18	22	20	67	50	45	89	79
% +B	13	14	29	1	28	21	18	86

Table 7 The % −A and % +B distortion values of the complexes measured using the in-plane angle data of Fig. 4(*d*)

	Complex							
	1	**5**	**2**	**6**	**7**	**8**	**3**	**4**
% −A	12	23	39	63	31	60	75	91
% +B	20	28	38	6	19	20	11	86

points are observed in the −A + B quadrant of the graph. There are no data points on the RTB ⟶ ± A or RTB ⟶ ± B route pathways. There is one data point **2** on the RTB ⟶ RSBP (−A + B) pathway, with two more data points, **4** and **5**, lying close by. Table 7 shows the % −A and % +B distortion values of the complexes calculated using the in-plane Cu–N(2) and Cu–N(4) distance data. The values are closely comparable to those in Table 6 using the corresponding in-plane angle data. In general, Tables 6 and 7 show that −A distortion dominates over +B route distortion. Data point **4** is exceptional because it shows both a large % −A and a large % +B distortion value, 91 and 86% respectively. It also explains why the Cu–N(2) distances of **6** and **3** are well above 2.092 Å, due to a significant −A route distortion and not to a −B route distortion.

General conclusions. The information obtained from the scatter-plot analysis of this series of eight [Cu(phen)$_2$Cl][Y] complexes can be summarised as follows.

(1) The distribution of the data points is not random, with respect to the RTB and RSBP data points. They involve a significant spread of 31° and 0.12 Å.

(2) The τ plot is consistent with a SBP distortion of the RTB CuN_4Cl chromophore, but with neither the RTB or RSBP structures present. Seven complexes have τ values in the range of 0.81–0.56. Data point, **4**, has an exceptional τ value of 0.19, which equates with an unusual TBDSBP stereochemistry for a [Cu(phen)$_2$Cl][Y] complex.

(3) The plot of α_3 *versus* α_1 shows data points lying on parallel correlations, with fixed α_2 values of 120 ± 5, 10 or 15°, suggesting the existence of preferred angles or 'magic angles', consistent with $\alpha_1 + \alpha_2 + \alpha_3 = 360°$, Table 4.

(4) The ±A and ±B axes of Fig. 1 can be superimposed on the plots. All data points lie in the −A + B section of the graphs. Tables 6 and 7 show the % −A and % +B distortion values of the complexes calculated from the in-plane angle and distance data and show that, in general, −A distortion is predominant over +B distortion. The tables also show that data point **4** is exceptional because of the large % values of both −A and +B distortion. The +A ⟶ RTB ⟶ − A pathway generates a novel −A or 'seesaw' stereochemistry.[18]

Possible interpretation of the ±A and ±B route distortions in terms of modes of vibration

The extensive range of the Cu–L distances and of the α_n angles, Table 3, 0.12 Å and 31°, respectively, have only been interpreted in terms of the ±A and ±B route distortions. It has been suggested earlier[1] that these routes may be understood, alternatively, in terms of the modes of vibration of the CuN_4Cl chromophore, Fig. 5. The symmetric, ν_{sym}, and asymmetric, ν_{asym}, modes of vibration of the CuN_4Cl chromophore, Fig. 5,

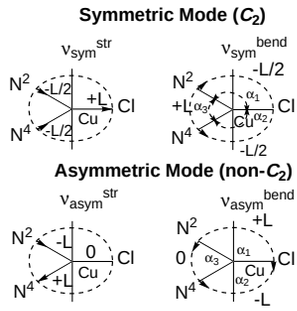

Fig. 5 The symmetric and asymmetric modes of vibration for the five-co-ordinate CuN_4Cl chromophore, including the relative magnitudes (L)[19,20]

both have stretching and bending components.[19,20] They predict variations in the in-plane parameters, α_{1-3}, Cu–Cl, Cu–N(2) and Cu–N(4), which show the largest ranges in distances and angles, Table 2. The symmetric mode of vibration has a two-fold axis of symmetry, so Cu–N(2) = Cu–N(4) and $\alpha_1 = \alpha_2$, and all six in-plane distances and angles are involved. The asymmetric mode of vibration does not have a two-fold axis of symmetry. Here only the Cu–N(2) and Cu–N(4) distances and the α_1 and α_2 angles are involved, with the Cu–Cl distance and the α_3 angle invariant. In the next section the [Cu(phen)$_2$Cl][Y] data are compared by scatter-plot analysis of the in-plane bond lengths and angles, to determine if the distribution of data points is random or determined by the ν_{sym} and ν_{asym} modes of vibration as the dominant modes of distortion of the CuN_4Cl chromophore, Fig. 5.

The first problem associated with this suggestion is that the effect of a single mode of vibration of the nuclear framework of the CuN_4Cl chromophore, of *ca.* 200 cm^{-1}, would only result in bond distance and angle changes of 0.005 Å and 1°, respectively.[21] These values are at least an order of magnitude too small to account for the observed changes, Table 3. Consequently, either a progression of 10–30 modes of vibration must be involved or the 'amplification factor'[22] of the pseudo-Jahn–Teller effect[23] must be in operation, with the possibility that the former accounts for the latter.

The most convincing evidence for the vibronic coupling model has been in accounting for the dynamic pseudo-Jahn–Teller distortion of the high-symmetry RTB $[CuCl_5]^{3-}$ anion, D_{3h} symmetry, to the lower-symmetry RSBP stereochemistry, C_{2v} or C_2 symmetry, with distortion *via* the ε′ mode of vibration[19,20,24,25] (equivalent to $\nu_{sym} + \nu_{asym}$), with C_2 symmetry along the three in-plane directions at 120° to each other. While the authors admit[19] that this model is only justified for small distortions, the above 'amplification factors'[22] or progressions could equally be operating to account for the larger distortions observed. If the same model is applied to the CuN_4Cl chromophore it must have the *effective* symmetry D_{3h} and ignores the presence of non-equivalent donor atoms and the effect of two chelate ligands. If this assumption can be accepted, then the ε′ mode of vibration, in D_{3h} symmetry, and the ν_{sym}^{str} and ν_{sym}^{bend} modes of vibration (C_2 symmetry) models are equivalent. However, we consider this too large an assumption and prefer the ν modes of vibration notation as it is chemically more informative than the ε mode notation. The highest possible symmetry for the CuN_4Cl chromophore is C_2, which is restricted to the Cu–Cl direction of the CuN_4Cl chromophore (±A route) and one that is quite distinct from the two ±B route distortions, which are related by a two-fold axis.

One of the most significant features of Fig. 4(*c*) is that two of the data points lie strictly along the +A ⟶ RTB ⟶ − A pathway, suggesting that the changes in the α_3 angle and Cu–Cl distance are closely linked. One such linking process suggests that the changes in these parameters is determined only by the

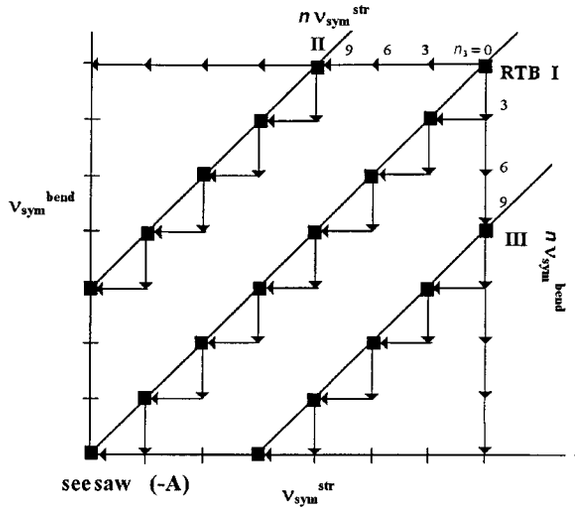

Fig. 6 Diagram illustrating how the linear and parallel pathways are formed by a progression of the coupled ν_{sym}^{str} and ν_{sym}^{bend} modes of vibration

underlying nuclear modes of vibration,[20,26] Fig. 5, suggesting a vibronic coupling mechanism.[23] A feature of the parameters of Fig. 4(*c*) is that the α_3 angle can only be changed by the ν_{sym}^{bend} mode of vibration and the Cu–Cl distance can only be changed by the ν_{sym}^{str} mode of vibration. If such modes operated separately from the RTB (point **I**) in Fig. 6, the former would only produce a vertical linear correlation of data points and the latter a horizontal correlation. While such limited correlations can be identified in Fig. 4(*c*), the most convincing correlation of two data points occurs at an angle of 34° to the Cu–Cl axis. The only way such a positive correlation can occur is if the two modes of vibration are strongly coupled (they both transform as the A_1 representation in C_{2v} symmetry or as A in C_2 symmetry), as shown in Fig. 6, to produce a stepped displacement. However, such a single displacement due to one quantum of each mode of vibration would still be too small to be observed on the scale of Fig. 4(*c*), namely, 0.005 Å and 1°. For the scale of the $+A \longrightarrow RTB \longrightarrow -A$ pathway in Fig. 4(*c*) to be observed, that is a change of 0.05 Å in the Cu–Cl distance and a change of 21° in the α_3 angle, a progression of 10–30 coupled vibrations must occur to account for the magnitude of the observed changes. Such a progression can be considered as plot of the structural pathway from the +A route to the −A route of Fig. 6, involving the coupled $\nu_{sym}^{str} + \nu_{sym}^{bend}$ modes of vibration, with the two data points representing two separate individual steps along the structural pathway, and each point characterised by a full single-crystal structure determination.

In order to explain the occurrence of the parallel correlations in Fig. 4(*c*), *n* modes of a **single** vibration, $\pm\nu$, where $n = 8$–10, must be involved in order that the parallel displacement can be observed, Fig. 6, **II** and **III**. This is then followed by a progression of the coupled modes, separate but parallel to the central linear correlation. This observation of linear and parallel correlations in the same plot, Fig. 4(*c*), is one of the best pieces of evidence for both structural pathways and parallel pathways and stems from the 'amplification factor'[22] in the pseudo-Jahn–Teller effect.[23]

The various plots also suggest that the directions of distortion from RTB to RSBP could be associated with the modes of vibration of the CuN_4Cl chromophore, Fig. 5. The ±A routes are associated with the ν_{sym}^{str} and ν_{sym}^{bend} modes of vibration and the ±B route distortions with the ν_{asym}^{str} and ν_{asym}^{bend} modes of vibration. However, as the actual data points rarely involve pure %A or %B contributions, all four modes are generally involved in the distortion of each complex, Tables 6 and 7.

Comparison of the [Cu(phen)$_2$Cl][Y] and [Cu(bipy)Cl][Y] series of complexes

The most obvious difference is in the range of τ values, with the phen complexes ranging from 0.81 to 0.19, while the bipy complexes[1] range from 1.00 to 0.53. In both series the bulk of the data points lie in the range τ 0.8–0.5, with the bipy series having four or five near RTB structures and the phen series involving an exceptional data point with a TBDSBP stereochemistry. Unfortunately, it is not possible to rationalise these differences in terms of the differences in structure of the bipy and phen ligands or in terms of the intramolecular non-bonding contacts of the $[Cu(chelate\ ligand)_2Cl]^+$ cations.

Implications

The four scatter plots of the eight [Cu(phen)$_2$Cl][Y] data points clearly suggest that the distribution with respect to the RTB and RSBP data points is not random, with some support for linear and parallel structural pathways. As there are no obvious differences in the local crystal environments between the extreme structures of complexes **1** and **4**, these extreme structures must reflect the structural pathways of the −A + B route of Fig. 1, which are determined by the effect of vibronic coupling. The precise stereochemistry displayed can be understood in terms of the possible linear combination of the coupled nuclear modes of vibration ν_{sym}^{str}, ν_{sym}^{bend}, ν_{asym}^{str} and ν_{asym}^{bend}. Each complex describes the local molecular stereochemistry of a point on the potential-energy surface of the structural pathway from RTB to RSBP, Fig. 1. The [Cu(phen)$_2$Cl][Y] data then represent the best evidence for the involvement of vibronic coupling to account for the structural consequences of the plasticity effect[27] in the series of cation distortion isomers[28] of the copper(II) ion. Of equal importance is the wide range of stereochemistry displayed by the **same** $[Cu(phen)_2Cl]^+$ cation, from near RTB, τ = 0.81, to TBDSBP, τ = 0.19. In the past, a number of accounts have been given[29–31] to describe the static geometries of the five-co-ordinate stereochemistries of **different** ML_5 chromophores and try to account for these changes in terms of the different bonding roles of the ligands present.[30] The present paper emphasises that, in the special case of the low-symmetry CuN_4X chromophore, vibronic coupling associated with the pseudo-Jahn–Teller effect,[23] can also produce the **same** range in stereochemistry of the five-co-ordinate ML_5 chromophore with the **same** set of ligands. The present study suggests a dynamic involvement of a number of the modes of vibration of the central chromophore to produce the changes associated with the movements about the potential-energy surface of the structural pathway in which individual points are characterised by single-crystal structure determinations of the same cation distortion isomers.[28]

Electronic properties of the [Cu(phen)$_2$Cl][Y] complexes

The polycrystalline electronic reflectance spectra of complexes **1**–**5** and **7** are shown in Fig. 7. For **1**, **2** and **5** a single $d \longrightarrow d$ transition occurs at 12 200, 12 100 and 12 200 cm^{-1}, respectively, with some evidence for a possible low-energy shoulder at 10 900, 10 500 and 10 800 cm^{-1}, respectively, consistent with near TB stereochemistries (τ = 0.81–0.73). The one-electron ground-state configuration is $d_{z^2} > d_{xy} \approx d_{x^2-y^2} > d_{xz} \approx d_{yz}$. The principal absorption may be assigned[1,32] as a $d_{xz} \approx d_{yz} \longrightarrow d_{z^2}$ transition, with the low-energy shoulder assigned as a $d_{x^2-y^2} \longrightarrow d_{z^2}$ transition.

The spectrum of complex **7**, τ = 0.66, shows a broad peak beginning to split into two. These two peaks involve energies of 10 200 and 13 300 cm^{-1} and appear to evolve from the single peak at 12 000 cm^{-1} for a RTB stereochemistry. The spectrum of **3**, τ = 0.56, which has an intermediate stereochemistry between RTB and RSBP, involves two clearly resolved peaks at 9800 and 13 700 cm^{-1}, with the higher-energy peak showing a

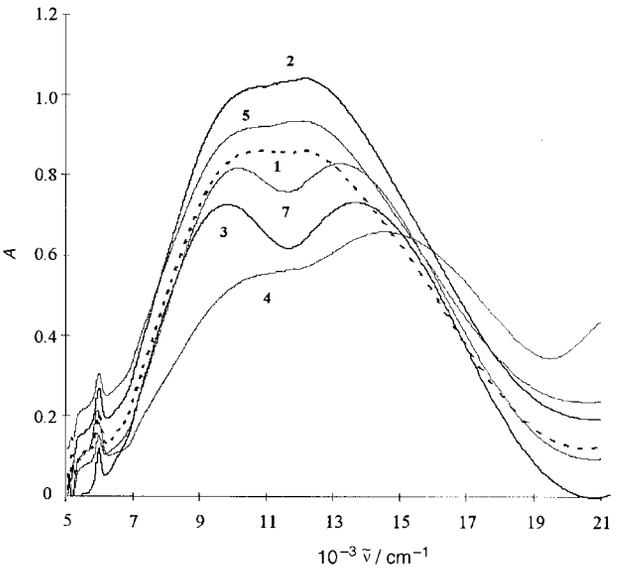

Fig. 7 Electronic reflectance spectra of some $[Cu(phen)_2Cl][Y]$ complexes

slightly greater intensity. The one-electron ground-state configuration is $d_{z^2} > d_{x^2-y^2} > d_{xy} > d_{xz} \approx d_{yz}$. The transitions may be assigned as the $d_{x^2-y^2} \longrightarrow d_{z^2}$ transition for the low-energy peak and the $d_{xz} \approx d_{yz} \longrightarrow d_{z^2}$ transition for the high-energy peak.

Complex **4**, $\tau = 0.19$, which has a TBDSBP stereochemistry, involves a high-energy, high-intensity peak at 14 500 cm^{-1}, with a low-intensity, low-energy shoulder at 11 500 cm^{-1}. The one-electron ground-state configuration is $d_{x^2-y^2} > d_{z^2} > d_{xy} > d_{xz} \approx d_{yz}$. The transitions may be assigned as the $d_{z^2} \longrightarrow d_{x^2-y^2}$ transition for the low-energy peak and the $d_{xz} \approx d_{yz} \longrightarrow d_{x^2-y^2}$ transition for the high-energy peak. This is consistent with the change in stereochemistry from near RTB to TBDSBP, the electronic criterion of stereochemistry[33] and emphasises the value of the electronic reflectance spectra, Fig. 7, in identifying the extreme stereochemistries in a series of cation distortion isomers, $[Cu(phen)_2Cl]^+$, along with the need to determine the structure of more than one isomer to establish both the range and a typical structure in such a series.

Acknowledgements

The authors acknowledge the award of an Irish Science and Technology Agency (EOLAS) grant for the diffractometer, EOLAS, Forbairt and University College Cork (U.C.C.) for Studentships (to G. M., P. N. and B. M.), data collection for complexes **1** and **2** by Professor M. McPartlin and Mr A. Bashall (University of North London), the Computer Bureau, U.C.C., for computing facilities, Professor G. M. Sheldrick, Drs P. Roberts, K. Henrick, A. L. Spek and P. McCardle for the use of their crystallography programs and the Microanalysis Section, U.C.C., for analysis.

References

1 Part 1, W. D. Harrison, D. M. Kennedy, M. Power, R. Sheahan and B. J. Hathaway, *J. Chem. Soc., Dalton Trans.*, 1981, 1556; Part 2, P. Nagle, E. O'Sullivan, B. J. Hathaway and E. Muller, *J. Chem. Soc., Dalton Trans.*, 1990, 3399.
2 H. Burgi and J. D. Dunitz, *Acc. Chem. Res.*, 1983, **16**, 153; J. D. Dunitz, *X-Ray Analysis and Structure of Organic Molecules*, Cornell University Press, London, 1979, ch. 7.
3 B. J. Hathaway, *Struct. Bonding* (*Berlin*), 1984, **57**, 55.
4 D. Boys, C. Escobar and S. Martinez-Carrera, *Acta Crystallogr., Sect. B*, 1981, **37**, 351.
5 A. K. Chilkevich, B. P. Ponomarev, P. P. Lyavrentjeu and L. O. Atoumjan, *Koord. Khim.*, 1987, **13**, 1532.
6 D. Boys, *Acta Crystallogr., Sect. C*, 1988, **44**, 1539.
7 D. T. Cromer and J. T. Waber, *International Tables for X-Ray Crystallography*, Kynoch Press, Birmingham, 1974, vol. 4, pp. 71, 148 (Present distributor, Kluwer Academic Publishers, Dordrecht).
8 G. M. Sheldrick, SHELX 76, program for X-ray crystal structure determination, University of Cambridge, 1976.
9 G. M. Sheldrick, SHELXS 86, program for X-ray crystal structure solution, University of Göttingen, 1986.
10 P. Roberts and G. M. Sheldrick, XANADU, program for the calculation of crystallographic data, University of Cambridge, 1979.
11 K. Henrick, PUBTAB, program to prepare and print crystallographic tables for publication, University of North London, 1980.
12 P. McCardle, XCAD, program for data reduction of CAD4 output, University College Galway, 1990.
13 A. L. Spek, PLUTON 92, program to prepare and print molecular structures, University of Utrecht, 1992.
14 I. M. Procter, B. J. Hathaway and P. Nicholls, *J. Chem. Soc. A*, 1968, 1678.
15 A. W. Addison, T. Nageswara Rao, J. Reedjik, J. van Rijn and G. C. Verschoor, *J. Chem. Soc., Dalton Trans.*, 1984, 1349.
16 F. Huq and A. C. Shapski, *J. Chem. Soc. A*, 1971, 1927.
17 G. Murphy, M. Brophy, B. Murphy, C. O'Sullivan and B. J. Hathaway, *Acta Crystallogr., Sect. C*, 1997, submitted for publication.
18 G. Murphy, C. Murphy, B. Murphy and B. Hathaway, following paper.
19 D. Reinen and M. Atanasov, *J. Chem. Phys.*, 1989, **136**, 27; *Magn. Reson. Rev.*, 1991, **15**, 167.
20 M. Bacci, *J. Chem. Phys.*, 1986, **104**, 191.
21 P. Brint, personal communication.
22 I. B. Bersuker, *Coord. Chem. Rev.*, 1975, **14**, 357.
23 I. B. Bersuker, *The Jahn–Teller Effect and Vibronic Interations in Modern Chemistry*, Plenum, New York, 1983.
24 D. Reinen, *Comments Inorg. Chem.*, 1983, **2**, 227.
25 D. Reinen, in *Vibronic Processes in Inorganic Chemistry*, ed. C. D. Flint, Kluwer, Dordrecht, 1989.
26 K. Nakamoto, *Infrared Spectra of Inorganic and Coordination Compounds*, 3rd edn, Wiley, New York, 1978.
27 J. Gazo, I. B. Bersuker, J. Garaj, M. Kabesova, J. Kohout, H. Langfeldorova, M. Melnik, M. Serator and F. Valach, *Coord. Chem. Rev.*, 1976, **21**, 253.
28 N. J. Ray, L. Hulett, R. Sheahan and B. J. Hathaway, *J. Chem. Soc., Dalton Trans.*, 1981, 1463.
29 E. L. Muetterties and L. T. Guggenberger, *J. Am. Chem. Soc.*, 1974, **96**, 1748.
30 R. R. Holmes and J. A. Deiters, *J. Am. Chem. Soc.*, 1977, **99**, 3318.
31 T. P. Auf der Heyde and H.-B. Burgi, *J. Am. Chem. Soc*, 1989, **28**, 3960, 3970, 3982.
32 B. J. Hathaway and D. E. Billing, *Coord. Chem. Rev.*, 1970, **5**, 143.
33 B. J. Hathaway, *J. Chem. Soc., Dalton Trans.*, 1972, 1192.

Received 26*th March* 1997; *Paper* 7/02291C